Enhancement of docetaxel solubility *via* conjugation of formulation-compatible moieties

Loan Huynh,[a] Jean-Christophe Leroux[b,c] and Christine Allen*[a]

Received 6th April 2009, Accepted 27th May 2009
First published as an Advance Article on the web 2nd July 2009
DOI: 10.1039/b906862g

Computer-based theoretical calculations were employed to direct the design of docetaxel conjugates with enhanced solubility in the internal phase of a nano-emulsion formulation. The theoretically-identified optimal docetaxel conjugates were synthesized by direct attachment of lauroyl moieties through an ester linkage to docetaxel. In comparison to docetaxel, the conjugates exhibited significantly improved solubility in oil, as predicted by our theoretical calculations. This contributed to high drug entrapment efficiencies (up to 97%) and a high drug loading capacity (5.7% w/w) for the docetaxel conjugates. The mono-substitution of an acyl group at C-2′ of docetaxel resulted in a conjugate with 37- to 46-fold lower cytotoxicity than that of the parent drug in two human cancer cell lines. Importantly, the activity exerted by the mono-substituted docetaxel on the cancer cells was due in part to the cytotoxicity of the parent drug that was released *via* hydrolysis of the ester bond between the lauroyl moiety and the drug under biologically relevant conditions. In contrast, di- and tri-substitution of acyl groups at C-2′, C-7 and/or C-10 of docetaxel resulted in non-hydrolysable conjugates that were found to be inactive. Overall, our results show that computer-based theoretical calculation is a promising strategy for guiding the enhancement of material–drug compatibility in formulation development. Also, these studies confirm that chemical modification of docetaxel for enhancement of material–drug compatibility should be limited to mono-substitution at C-2′ and result in a prodrug that is hydrolysable at a moderate rate under biologically relevant conditions.

Introduction

It has been reported that about 40% of the small molecules that are emerging as new drug candidates are hydrophobic.[1] Full exploitation of the therapeutic potential of hydrophobic drugs relies on their solubilization in a formulation or requires an advanced delivery system. However, low drug loading levels (*i.e.* low drug to material ratio) and poor drug retention in the delivery system following administration remain serious problems.[2,3] In order to address these challenges, contemporary efforts are focused on optimizing the compatibility between the drug and the excipient (*i.e.* polymer or lipid) that forms the core of the delivery system.[4–7] Optimization of the compatibility between the hydrophobic drug and core-forming material has been shown to result in significant improvements in formulation stability, drug loading capacity and drug retention.[7]

Several strategies have been successfully utilized in order to enhance material–drug compatibility; of particular note are the following three approaches. First, one may pre-screen a library of materials against the drug of interest using semi-empirical and computational methods in order to identify the best material–drug pair.[1,8–10] Second, chemical modification of the core-forming material of the delivery system has the potential to increase the suitability of the core as a microenvironment for solubilization of a specific drug (*e.g.* NK911 – a formulation of doxorubicin,[6] and NK105 – a formulation of paclitaxel (PTX)[5]). Third, the drug molecules may be chemically modified or conjugated to generate a prodrug that has increased solubility, loading and/or retention in a specific formulation. For example, a study by Lundberg *et al.* demonstrated that the prodrug PTX-oleate is significantly more soluble in a cholesterol microemulsion formulation than PTX.[7] Also, the prodrug PTX-docosahexanoic acid[11] (*i.e.* Taxoprexin®) was found to have a higher solubility than unmodified PTX in the conventional formulation of PTX that is known as Taxol® and formed from 10% Cremophor EL-P/10% ethanol/80% saline.[11] Taxoprexin® has entered phase III clinical development, targeting patients with locally advanced or metastatic NSCLC.[12]

Currently, the taxanes, namely PTX and docetaxel (DTX), are the most widely used hydrophobic drugs for the treatment of cancer.[13,14] Indeed PTX, in the commercially available formulation Taxol®, is approved for first-line treatment of various cancers such as ovarian, breast, and non-small-cell lung. The commercially available formulation of DTX, known as Taxotere®, is approved for first-line treatment of prostate, gastric, lung, breast and head and neck cancers.[13–16] PTX and DTX exert their cytotoxic effect by binding β-tubulin and inhibiting microtubule depolymerisation, which leads to cell cycle arrest.[14,17] While PTX and DTX are structurally similar, and several pre-clinical and clinical studies have shown that DTX is at least as effective as PTX,[13,14,18–22] their pharmaceutical characteristics have important distinctions. In comparison to PTX, DTX binds microtubules with greater affinity,[14] and *in vitro* studies have revealed that DTX is more

[a]*Leslie Dan Faculty of Pharmacy, University of Toronto, 144 College Street, Toronto, Ontario, M5S 3M2, Canada. E-mail: cj.allen@utoronto.ca; Fax: 416-978-8511; Tel: 416-946-8594*
[b]*Institute of Pharmaceutical Sciences, ETHZ, 8093 Zürich, Switzerland*
[c]*Faculty of Pharmacy, University of Montreal, Montreal, Québec, H3C 3J7, Canada*

cytotoxic.[17,23] However, the commercially available formulation of DTX (*i.e.* Taxotere®)[17] has side-effects that are caused by the polysorbate 80 formulation vehicle, such as acute hypersensitivity reactions and vesicular degeneration.[24–26] There is therefore an impetus to develop new formulations of DTX that are formed from safer excipients or materials.

With the intention of developing a safer delivery material to replace polysorbate 80, we recently generated nanoemulsion (NE)/nanocapsule formulations stabilized by a non-toxic poly(ethylene glycol) (PEG) derivative (*viz.* Solutol® HS 15[27]) that was shown to circulate for prolonged periods *in vivo* and accumulate preferentially at the tumor site.[28,29] The inner phase of this NE included FDA-approved medium chain triglycerides[30] (*i.e.* caprylic/capric triglyerides; Labrafac™). However, the drug loading capacity of this NE formulation for DTX was not optimal; therefore large volumes of the NE formulation would need to be administered in order to achieve therapeutic drug levels. In order to address this deficiency, this study pursues the chemical modification of DTX in order to improve the compatibility between the drug and the inner phase of the NE formulation.

In another article, we described both molecular dynamics and semi-empirical methods for estimating the solubility of DTX in various pharmaceutical excipients and validated the methods experimentally.[9] In this study, we employed a similar computational method to direct the chemical modification of DTX. The optimal DTX conjugates, identified by computer simulation, were synthesized, characterized and evaluated in terms of solubility in Labrafac™. NE formulations of the DTX conjugates were then prepared and investigated *in vitro* in terms of drug entrapment efficiency and stability. The experimental studies on DTX conjugates demonstrate significant improvements in solubility, drug loading capacity and entrapment efficiency in the NE formulation. Evaluation of the *in vitro* cytotoxicity of the conjugates in SKOV-3 and H460 cancer cells revealed a marked decrease in the activity of DTX conjugates relative to DTX. Only the mono-substituted DTX conjugate was slowly hydrolyzed *in vitro*, cleaving the conjugated moiety from the parent drug and thus alleviating the conjugation-based inhibition of cytotoxicity, which is all but complete. Therefore, the hydroxyl group at C-2′ of DTX was identified as the optimal group for *direct* chemical modification of the drug to produce a conjugate with enhanced solubility in the formulation and capacity for regeneration of the biological activity of the drug. Interestingly, the good agreement between the computational and the experimental solubility and hydrophobicity data suggests a bright future for theoretically-guided prodrug development of hydrophobic drugs.

Results and discussion

Theoretical hydrophobicity and solubility parameters

Lipidic nanoformulations that contained Labrafac™ as the core component have been shown to be stable *in vivo* with a prolonged circulation time and significant accumulation in solid tumors.[28,29] However, administration of large volumes of this emulsion would be required in order to achieve therapeutic drug levels due to the limited drug loading capacity of the NE formulation for DTX. Replacement of the inner phase of the NE with other excipients resulted in either less drug loading (*i.e.* poor solubility)[9] or serious toxic side-effects.[34] In light of the fact that the extent of drug loading and retention can be significantly improved by increasing the compatibility between the drug and the core of the delivery system,[8,10,37] we set out to investigate the conjugation of DTX to saturated fatty acid moieties that are structurally similar to Labrafac™ in terms of theoretical octanol-to-water partition coefficients ($\log P_{o/w}$) and Hildebrand solubility parameters (δ_{HIL}).

The $\log P_{o/w}$ and δ_{HIL} values of DTX, DTX conjugates and Labrafac™ were determined by computer simulation (Table 1). The δ_{HIL} of Labrafac™ (*i.e.* mainly a mixture of tricaprin and tricaprylin) is an average of the δ_{HIL} of tricaprylin ($\delta = 17.30$ $(J/cm^3)^{1/2}$) and tricaprin ($\delta_{HIL} = 17.80$ $(J/cm^3)^{1/2}$). For each drug–Labrafac™ pair, the difference between the δ_{HIL} of drug and δ_{HIL} of Labrafac™ ($\Delta\delta_{HIL}$) was calculated in order to estimate their relative miscibility. A lower value of $\Delta\delta_{HIL}$ for a specific drug–Labrafac™ pair is predicted to result in a higher solubility for the drug in Labrafac™. A higher value for the calculated $\log P_{o/w}$ is indicative of a more lipophilic drug and greater degree of compatibility between the drug and the oil phase. Importantly, based on the $\log P_{o/w}$ values for a total of ten compounds (Table 1), a linear relationship between the calculated $\log P_{o/w}$ values and the total number of carbon atoms in the acyl chains conjugated to DTX was obtained ($R^2 = 0.997$). The relationship was:

$$\log P_{o/w} = 0.44 \times (\text{no. carbon atoms in all acyl chains conjugated to DTX}) + \log P_{o/w}(\text{DTX}) \quad (1)$$

According to this relationship, each carbon atom in the attached acyl chain contributes approximately 0.44 ± 0.01 to the $\log P_{o/w}$ value for the DTX conjugate. As shown in Table 1, lower $\Delta\delta_{HIL}$ and greater $\log P_{o/w}$ values were obtained for DTX conjugated with longer hydrocarbon chains and/or more lipophilic side chains per drug molecule.[9] Studies have shown that the toxicity of fatty acids in Jurkat (T-lymphocyte) and Raji (B-lymphocyte) human cell lines decreased when the hydrocarbon chain length was decreased.[38] The tolerable concentration of lauric acid (C12:0) in human cell lines was quite high (*i.e.* 200 μM)[38] in comparison to the cytotoxicity of DTX in a range of human tumor cell lines (0.13 nM to 24 nM).[39] Furthermore, Immordino *et al.* reported that the interaction of a lipophilic prodrug with a liposome bilayer increased when the acyl chain of the prodrug penetrated into the lipid bilayer and completely overlapped with the hydrophobic tails of phospholipids, thus improving the stability of the liposome.[40] For these reasons, DTX conjugates with laurate moieties (C12:0, Table 1) were synthesized in order to produce conjugates with relatively non-toxic acyl chains that allow for full overlap with Labrafac™ (*i.e.* capric/caprylic glycerides), and yet have relatively moderate molecular weights and $\log P_{o/w}$ values.

Characterization of DTX conjugates

In this study, DTX was mono, di and trisubstituted with laurate moieties using a direct and efficient method that produced the DTX conjugates in high yield. The lauroyl chloric acid group of the fatty acid was directly conjugated to the hydroxyl (OH) group of DTX in a single step. Site-specific conjugation of fatty acid moieties to the OH groups of DTX was achieved by variation of the temperature during the reaction procedure.

The conjugation of the fatty acid moieties to DTX was confirmed by ^{1}H-NMR (Fig. 1). The ^{1}H NMR chemical shifts

Table 1 Docetaxel and candidate docetaxel conjugates. The octanol-to-water partition coefficients ($\log P_{o/w}$) and solubility parameters (δ_{HIL}) were calculated using QSAR+ and C2.Synthia, respectively

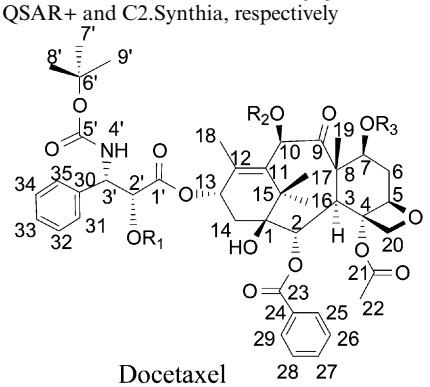

Mono-substituted-DTX: $R_2 = R_3 = H$, $R_1 =$ 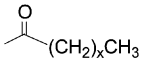

Di-substituted-DTX: $R_3 = H$, $R_1 = R_2 =$ 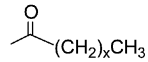

Tri-substituted-DTX: $R_1 = R_2 = R_3 =$ 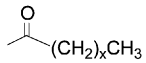

Labrafac™: y = 6 (tricaprylin)
y = 8 (tricaprin)

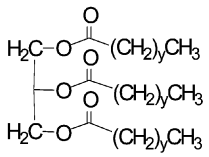

		Mono-substituted			Di-substituted			Tri-substituted		
		C10:0	C12:0	C14:0	C10:0	C12:0	C14:0	C10:0	C12:0	C14:0
	Docetaxel	x = 8	**x = 10**	x = 12	x = 8	**x = 10**	x = 12	x = 8	**x = 10**	x = 12
MW (g/mol)	**807.9**	962.1	**990.2**	1018.2	1144.4	**1172.5**	1228.6	1298.7	**1354.8**	1439.0
$\log P_{o/w}$	**2.45**	6.69	**7.60**	8.51	11.84	**12.75**	14.57	16.08	**17.90**	20.64
δ_{HIL} $(J/cm^3)^{1/2}$	**24.22**	22.66	**22.49**	22.33	21.44	**21.33**	21.13	20.65	**20.50**	20.30
$\Delta\delta_{HIL}$[a]	**6.67**	5.11	**4.94**	4.78	3.89	**3.78**	3.58	3.1	**2.95**	2.75

[a] $\Delta\delta_{HIL} = |\delta_{HIL-drug} - \delta_{HIL-Labrafac™}|$. The δ_{HIL} of Labrafac™ is 17.55, which is an average of δ_{HIL} values for tricaprylin ($\delta_{HIL} = 17.30$) and tricaprin ($\delta_{HIL} = 17.80$).

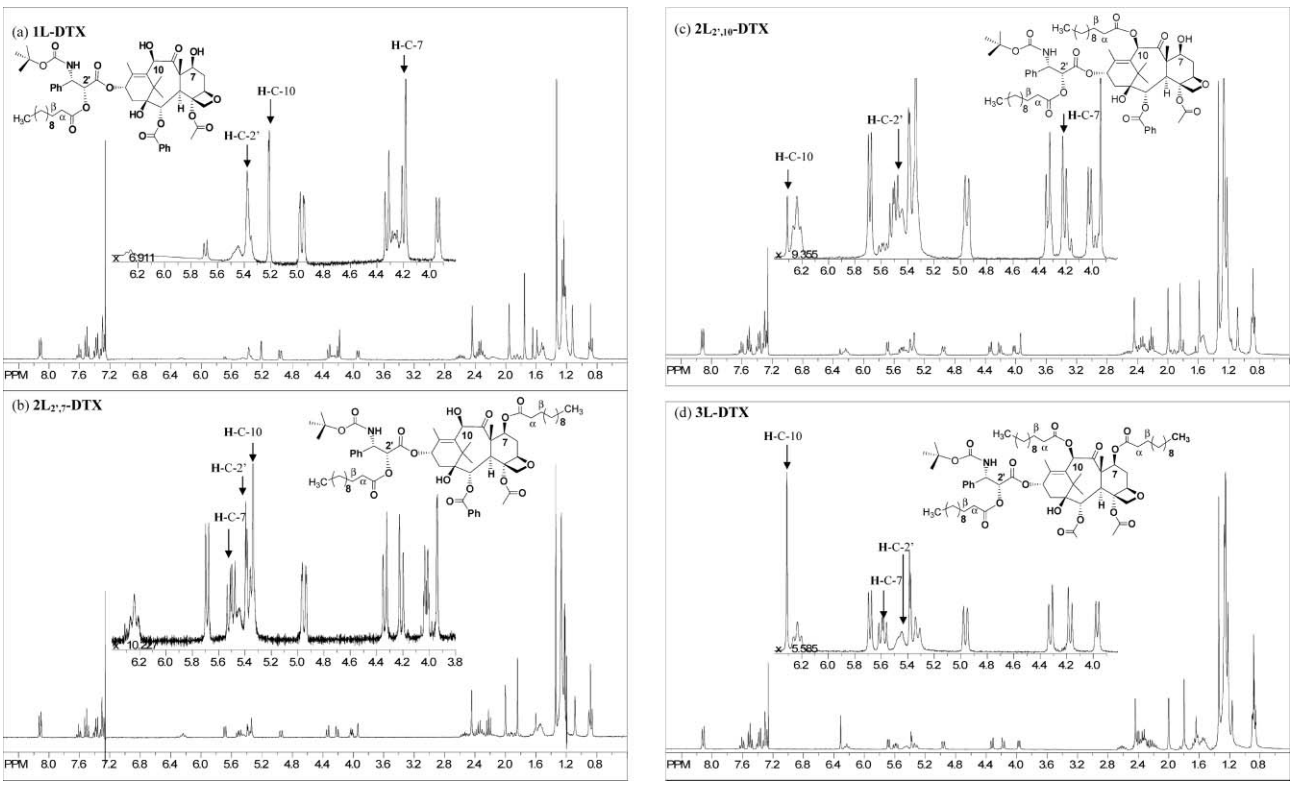

Fig. 1 ^{1}H NMR spectra of (a) **1L-DTX**, (b) **$2L_{2',7}$-DTX** (c) **$2L_{2',10}$-DTX** and (d) **3L-DTX**.

for the conjugated fatty acid moieties on DTX conjugates are recorded in Table 2. The proton intensities are in accordance with the structure of the drugs. The ^{1}H shifts for DTX and DTX conjugates were comparable to those reported previously for DTX and DTX derivatives.[41] The ^{1}H proton chemical shifts for the hydroxyl hydrogens at the C-2′ (*H*O-C-2′, 3.35 ppm), C-7 (*H*O-C-7, 1.50 ppm) and C-10 (*H*O-C-10, 4.20 ppm) atoms on DTX disappeared following conjugation of the fatty acid

Table 2 ^{1}H NMR data for docetaxel, **1L-DTX**, **2L$_{2',7}$-DTX**, **2L$_{2',10}$-DTX** and **3L-DTX**

Position[b]	^{1}H	Docetaxel	**1L-DTX**	**2L$_{2'-10}$-DTX**	**2L$_{2'-7}$-DTX**	**3L-DTX**
2	1H	5.68 (d, 7.1)	5.69 (d, 7.2)	5.69 (d, 7.1)	5.69 (d, 7.0)	5.68 (d, 7.0)
3	1H	3.91 (d, 7.0)	3.94 (d, 7.3)	4.02 (d, 7.1)	4.02 (d, 7.0)	3.97 (d, 7.0)
5	1H	4.94 (dd, 9.7, 2.1)	4.96 (dd, 9.6, 2.2)	4.95 (dd, 9.7, 2.2)	4.95 (dd, 9.7, 2.2)	4.95 (dd, 9.7, 1.6)
6	Ha	2.59 (dt, 3.2, 7.2)	2.59 (dt, 3.3, 7.4)	2.53 (ddd, 4.7, 9.2, 17.2)	2.62 (dt, 2.7, 7.3)	2.62 (dt, 2.5, 7.1)
6	Hb	1.85 (m)	1.85 (m)	1.92 (m)	1.92 (m)	1.76 (m)
7	1H	4.24 (m)	4.26 (m)	4.19 (m)	5.59 (m)	5.59 (m)
	OH	1.57 (br)	1.53 (br)	1.54 (br)	—	—
10	1H	5.20 (d, 1.6)	5.21 (d, 1.4)	6.31 (s)	5.34 (d, 1.20)	6.31 (s)
	OH	4.20 (d, 1.7)	4.18 (d, 1.4)	—	3.94 (d, 1.6)	—
13	1H	6.22 (t, 8.6)	—	6.24 (t, 8.8)	6.24 (t, 8.8)	6.23 (t, 8.8)
14	Ha	2.27 (d, 9.2)	2.34 (d, 8.2)	2.35 (d, 8.6)	2.35 (d, 8.7)	2.28 (d, 11.45)
16	3H	1.24 (s)	1.22 (s)	1.22 (s)	1.22 (s)	1.22 (s)
17	3H	1.13 (s)	1.12 (s)	1.09 (s)	1.09 (s)	1.17 (s)
18	3H	1.85 (s)	1.96 (s)	2.00 (s)	2.00 (s)	2.00 (s)
19	3H	1.76 (s)	1.75 (s)	1.84 (s)	1.84 (s)	1.80 (s)
20	Ha	4.32 (d, 8.5)	4.33 (d, 8.4)	4.34 (d, 8.4)	4.34 (d, 8.4)	4.32 (d, 8.3)
	Hb	4.19 (d, 8.5)	4.20 (d, 8.4)	4.21 (d, 8.6)	4.21 (d, 8.7)	4.17 (d, 8.4)
22	3H	2.37 (s)	2.44 (s)	2.44 (s)	2.44 (s)	2.42 (s)
25 and 29	2H	8.11 (d, 7.3)	8.12 (d, 7.1)	8.12 (d, 7.1)	8.12 (d, 7.1)	8.12 (d, 7.1)
26 and 28	2H	7.50 (t, 7.3)	7.50 (t, 7.2)	7.50 (t, 7.3)	7.50 (t, 7.2)	7.50 (t, 7.2)
27	1H	7.61 (t, 7.5)	7.61 (t, 7.2)	7.61 (t, 7.4)	7.61 (t, 7.4)	7.61 (t, 7.4)
31 and 35; 32 and 34	4H	7.35–7.42 (m)	7.34–7.43 (m)	7.35–7.43 (m)	7.35–7.42 (m)	7.35–7.42 (m)
33	1H	7.32 (m)	7.30 (m)	7.30 (m)	7.30 (m)	7.31 (m)
2′	1H	4.62 (br)	5.44 (br)	5.44 (br)	5.44 (br)	5.44 (br)
	OH	3.34 (d, 5.4)	—	—	—	
3′	1H	5.26 (d, 8.6)	5.36 (d, 9.5)	5.34 (d, 9.6)	5.35 (d, 7.4)	5.32 (d, 9.9)
4′	1H	5.42 (d, 9.4)	5.37 (d, 2.9)	5.39 (d, 2.8)	5.39 (d, 3.1)	5.38 (d, 3.2)
7′, 8′, 9′	9H	1.34 (s)	1.33 (s)	1.34 (s)	1.34 (s)	1.34 (s)
Laurate side chain(s)						
CH_3[c]	# L × 3H		0.88 (m)	0.88 (m)	0.88 (m)	0.88 (m)
$(CH_2)_8$[c]	# L × 8 × 2H		1.25 (m)	1.27 (m)	1.24 (m)	1.24 (m)
C_β at C-2′	2H		2.34 (m)	2.35 (m)	2.35 (m)	2.32 (m)
C_β at C-7	2H			2.22 (t, 7.3)	2.22 (t, 7.5)	2.22 (m)
C_β at C-10	2H					2.22 (m)
C_α[c]	# L × 2H		1.53 (m)	1.59 (m)	1.54 (m)	1.45–1.70 (m)

[a] Chemical shifts are in ppm; coupling constants are in Hz. Multiplicities are as follows: s: singlet; d: doublet; dd: doublet of doublets; t: triplet, dt: doublet of triplets; m: multiplet; br: broad. [b] Refers to the structural formula given in Table 1. [c] Total number of H = (number of laurate side chains × number of hydrocarbon groups) × 2H.

moieties. Furthermore, the ^{1}H chemical shift for the hydrogens connected to C-2′ (*H*C-2′, 4.62 ppm), C-7 (*H*C-7, 4.24 ppm) and C-10 (*H*C-10, 5.20 ppm) atoms resonated at lower field strengths due to the conjugation.

For example, as shown in Fig. 1a, the ^{1}H-NMR for **1L-DTX** verified the conjugation of lauroyl chloride to the OH group at the C-2′ atom, by the absence of the peak at 3.35 ppm (*H*O-C-2′) and a shift in the peak at 4.62 ppm (br) to 5.45 ppm (br). The calculated mass of **1L-DTX** (989.5) agreed with the data obtained by ESI analysis, (990.5 [M + H$^+$], 1007.5 [M + NH_4^+] and 1012.5 [M + Na$^+$]).

As demonstrated in the ^{1}H-NMR for **2L$_{2',7}$-DTX** (Fig. 1b), in addition to the observations in the ^{1}H-NMR for **1L-DTX**, the peak at 1.50 ppm (*H*O-C-7, br) was not detected whereas the peak at 4.24 ppm (m, *H*C-7) was reallocated to 5.59 ppm (q), verifying the formation of **2L$_{2',7}$-DTX**. The formation of **2L$_{2',10}$-DTX** was demonstrated by ^{1}H-NMR based on the disappearance of the peak at 4.20 ppm (d, *H*O-C-10) and a shift in the peak corresponding to the hydrogen at the C-10 position from 5.20 ppm (d) to 6.31 ppm (d). The mass spectra of **2L-DTX** obtained by ESI analysis showed a protonated molecule [M + H$^+$] at 1172.7 that agreed with the calculated mass (1171.7).

The above NMR observations for **1L-DTX**, **2L$_{2',7}$-DTX** and **2L$_{2',10}$-DTX** were also found for **3L-DTX**, confirming the formation of **3L-DTX**. The calculated mass of **3L-DTX** was 1353.9, which agrees with the mass obtained by ESI, *i.e.* 1371.9 [M + NH_4^+].

Previous studies on the conjugation of PTX to hyaluronic acid have revealed that hyaluronic acid is preferentially conjugated to the OH-C-2′ group in PTX, rather than the more sterically hindered OH-C-7 group.[42–44] Therefore, it was expected that the conjugation of DTX to fatty acid moieties would preferentially occur at the OH-C2′ group of DTX. Amongst secondary conjugation sites, the OH-C-7 group is predicted to have slightly higher chemical reactivity toward the conjugation of a fatty acid than the OH-C-10 group. In fact, the formation of **2L$_{2',7}$-DTX** product was found to be approximately 4.5 times greater than **2L$_{2',10}$-DTX**. These results show that the OH-C-2′ group is the most favourable conjugation site for fatty acid moieties, followed by the OH-C-7 group and, finally, the more sterically hindered OH-C-10 group.

Experimental lipophilicity and solubility

In order to validate the results obtained by computer simulation, the relative lipophilicity of DTX and conjugates were determined based on their retention time obtained from the HPLC chromatograms and compared to the theoretically calculated $\log P_{o/w}$ values. It is worth noting that a C_{18} reverse-phase column was used for HPLC analysis, hence under similar conditions less lipophilic molecules are eluted earlier than more lipophilic molecules. According to the retention time of DTX and conjugates obtained from HPLC using 2-propanol:acetonitrile:water (40:45:15, v/v/v) as mobile phase, DTX ($R_T = 2.8$ min) was the least lipophilic molecule followed by **1L-DTX** ($R_T = 5.1$ min), **$2L_{2',10}$-DTX** ($R_T =$ 20.5 min), **$2L_{2',7}$-DTX** ($R_T = 22.4$ min) and then **3L-DTX** ($R_T >$ 60 min). Similarly, the theoretically calculated $\log P_{o/w}$ values increased with number of conjugated acyl chains. Therefore, the relative lipophilicity of each of the conjugates was found to be in good agreement with the $\log P_{o/w}$ values, and may be tuneable by varying the acyl chain length and the number of side chains attached to DTX (eq. 1).

The experimental solubility of DTX and DTX conjugates were determined and employed to validate the results obtained by computer simulation. In comparison to the solubility of DTX in Labrafac™, only the relative solubilities of the DTX conjugates were determined due to their high solubility in Labrafac™ (27% w/w of **1L-DTX**, 34% w/w of **2L-DTX** or **3L-DTX** in the Labrafac™ unsaturated solution). As listed in Table 3, the relative solubility of the DTX conjugates in Labrafac™ (>345 mg/mL DTX equivalent) is more than eight-fold higher than the solubility of unmodified DTX in Labrafac™ (43.7 mg/mL or 4% w/w of DTX in Labrafac™ saturated solution).[9] It is well known that the solubility of a compound is based on the concept of "like dissolves like".[45] In comparison to unmodified DTX, DTX conjugates (*i.e.* **1L-DTX**, **2L-DTX**, **3L-DTX**) are more lipophilic as indicated by their higher $\log P_{o/w}$ values and longer retention times observed by HPLC analysis. Therefore, the DTX-conjugates have a greater solubility in Labrafac™. In addition, the significant enhancement in the miscibility of the DTX conjugates is attributed to the similarity of the chemical structure of Labrafac™ and the laurate moieties that are conjugated to DTX (Table 1). In comparison to the previously reported solubility for DTX in various triglycerides[9], the solubility of DTX conjugates in Labrafac™ is significantly greater than the solubility of DTX in tributyrin (108 mg/mL) and Labrafac™ (43.7 mg/mL).

Table 3 Solubility and cytotoxicity of docetaxel (DTX) and DTX conjugates

DTX or DTX conjugates	Solubility[a] (mg/mL)	IC_{50}[b] (nM)	
		SKOV-3	H460
DTX	43.7 ± 0.5	1.8 ± 0.2	1.5 ± 0.7
1L-DTX	> 368 (300)	82 ± 16	56 ± 3
$2L_{2',7}$-DTX	> 500 (345)	$>2\times10^5$	$>2\times10^5$
3L-DTX	> 500 (298)	$>2\times10^5$	$>2\times10^5$

[a] Values in parentheses are equivalent concentration of DTX. [b] Data are presented as mean of DTX equivalent ± SD (n = 3). The chemical structure of **1L-DTX** (mono-substituted), **$2L_{2',7}$-DTX** (di-substituted) and **3L-DTX** (tri-substituted) are shown in Table 1 with x = 10.

Stability, drug loading and entrapment efficiency

NE formulations, outlined in Table 4, were prepared with low (*i.e.* formulation A) and high (*i.e.* formulation B) initial amounts of DTX or DTX equivalent. The amount of DTX or DTX equivalent initially added in **DTX-A** (formulation of DTX), **1L-DTX-A** (formulation of **1L-DTX**) and **2L-DTX-A** (formulation of **$2L_{2',7}$-DTX**) formulations was 0.6% by weight of the NE (*i.e.* 100% × initial weight of DTX or DTX equivalent ÷ the total mixture of Solutol® and Labrafac™). The **DTX-B** formulations were prepared initially with 1.2% by weight of DTX per mL of the NE, whereas the **1L-DTX-B** and **2L-DTX-B** formulations were initially prepared with 5.7% by weight of DTX equivalent per mL of the NE.

The stability of the NE formulations was observed by microscopic analysis. As discussed previously, the amount of drug loaded in the NE formulations depends on the solubility or miscibility of the drug in Labrafac™, which is the internal phase of the NE. Super-saturation of the drug in the NE formulations can lead to drug crystallization or precipitation, which was observed by microscopic analysis for **DTX-B** formulation. Drug-loaded NEs were in the range of 167 to 206 nm in diameter and stable over 24 h of storage at room temperature as determined by DLS. Following 48 h of storage at room temperature, DLS analysis of the NEs revealed bimodal population distributions with diameters of 180–250 nm and 300–500 nm for each population.

Table 4 Composition and properties of nano-emulsion formulations[a]

Formulation	DTX or DTX equiv. added[b] (mg)	DTX or DTX equiv. loaded[c] (% w/w)	Drug EE by ultracentrifuge (%)	Drug EE by dialysis (%)	Diameter (nm)	Polydispersity
NE control	0	—	—	—	198 ± 3	0.16 ± 0.20
DTX-A	15.0 (13.4)	0.6 (0.5)	90 ± 3	81 ± 6	199 ± 12	0.68 ± 0.88
DTX-B	30.0 (2.9)	1.2 (0.1)	10 ± 1	7 ± 1	182 ± 26	0.17 ± 0.04
1L-DTX-A	15.0 (13.8)	0.6 (0.6)	92 ± 4	80 ± 4	203 ± 7	0.19 ± 0.02
1L-DTX-B	150.0 (133.4)	5.7 (5.1)	89 ± 6	78 ± 3	184 ± 9	0.17 ± 0.03
2L-DTX-A	15.0 (14.6)	0.6 (0.6)	97 ± 1	85 ± 5	167 ± 9	0.15 ± 0.01
2L-DTX-B	150.0 (137.1)	5.7 (5.2)	91 ± 1	85 ± 3	206 ± 5	0.18 ± 0.03

[a] Nanoemulsion (NE) samples were prepared in triplicate. Constant amounts of Labrafac™ (1485 mg, 2.9 mmol), Solutol® (990 mg, 1 mmol) and NaCl 0.9 (w/v, 12.46 mL) were added to each NE formulation. [b] The amount of docetaxel (DTX) or DTX equivalent initially added and actually loaded (values in parentheses). [c] The percent of DTX equivalent initially added and actually loaded (values in parentheses) was determined as the weight percentage of DTX equivalent relative to the total weight of NE (drug, Labrafac™ and Solutol®) excluding the dispersion media. (d) Drug entrapment efficiency (EE) was calculated as the percentage of drug actually loaded relative to total drug initially added.

The drug loading and EEs were determined using the ultracentrifugation and dialysis methods that have been validated as efficient methods for measuring drug EE in parenteral emulsion, liposome and micelle formulations.[35,46] The molecular weight cutoff of the dialysis membrane (10 kDa) only allows for diffusion of the free DTX or DTX conjugates. Following dialysis, the drug entrapped NE in the dialysis bag was collected and analyzed by HPLC. In comparison, the ultracentrifugation method allows non-entrapped drug and the dispersion medium from the outer chamber to pass through a filter (molecular weight cutoff 10 kDa). Following ultracentrifugation, the drug entrapped NE in the supernatant and the dispersion medium were collected in separate chambers and analyzed by HPLC. In comparison to the drug EE obtained with the ultracentrifugation method, the EE measured using the dialysis method was 3–12% lower. The lower drug EE obtained from the dialysis method can be attributed to additional loss of entrapped drug that occurs following loss of the free drug and the equilibration process.[35]

About 90% of DTX was entrapped in the emulsion when the initial amount of drug added was 0.6% by weight (**DTX-A** formulation). Non-entrapped DTX was detected in the dispersion media at a concentration of 6 μg/mL. The drug loading and EE of DTX-loaded NEs significantly decreased when the initial amount of DTX added was doubled, indicating that the maximum drug loading capacity was reached with the **DTX-A** formulation. Furthermore, the drug precipitate in the **DTX-B** formulation was effectively separated from the NE sample, hence further indicating the validity of the dialysis and ultracentrifugation methods for the measurements of drug loading and EE.

As discussed previously, the conjugation of fatty acid to DTX results in a significant improvement in miscibility between the drug and Labrafac™, as well as an increase in drug loading and drug EE in the NE formulations, in comparison to unmodified DTX. According to the results obtained from the ultracentrifugation method, with an additional drug loading of 0.6% by weight, the percentage of DTX conjugates entrapped in the NE formulations were 92% (**1L-DTX-A** formulation) and 97% (**2L-DTX-A** formulation). As the initial drug added increased to 5.7% by weight in the **1L-DTX-B** and **2L-DTX-B** formulations, approximately 89–91% of DTX conjugates were entrapped in the NE. The concentration of non-entrapped **2L-DTX** and **1L-DTX** in the dispersion media was in the range of 1.0 μg/mL to 1.6 μg/mL. Furthermore, small amounts of non-entrapped DTX conjugates (0.06–0.6% w/w of the added DTX conjugates) were hydrolyzed and converted to DTX in the dispersion media as detected by HPLC analysis. Analysis of the entrapped NE formulations of **1L-DTX** and **2L-DTX** revealed no DTX. The final concentrations of **1L-DTX** and **2L-DTX** were 89 mg and 91 mg of DTX equivalent per mL of Labrafac™ in the **1L-DTX-B** and **2L-DTX-B** formulations, respectively.

Many studies have reported that the drug loading capacity and EE of formulations are related to the solubility and hydrophobicity of the drug.[37,47,48] In comparison to DTX, the actual drug loading of the DTX conjugates in the **1L-DTX-B** and **2L-DTX-B** formulations (Table 4) is approximately 10-fold higher in terms of DTX equivalent. This enhancement in the drug loading of the DTX conjugates can be attributed to the increase in the lipophilicity and the miscibility between the DTX conjugates and Labrafac™, in comparison to DTX. The loading of the DTX conjugates in the PEG-based NE formulations is also approximately five times higher than the loading of a PTX-oleate derivative in a cholesterol microemulsion.[7] In the current research, the concentration of drug solubilized was 4.5 mol% (DTX equivalent) relative to the total moles of Labrafac and Solutol HS15, while in the previous study a loading of 0.9 mol%.[7] (PTX equivalent relative to total moles of lipid and surfactant) was obtained for PTX-oleate in the cholesterol microemulsion.[7] Furthermore, the loading level of the DTX conjugates in the NE formulations were comparable to the levels achieved for PTX in micelle formulations (*i.e.* 1% to 4% by weight).[47,49]

In vitro cytotoxicity and hydrolysis of DTX conjugates

In order to maximize drug efficiency, the chemical modification of a taxane to improve solubility should not lead to a pronounced decrease in the activity of the drug at the tumor site.[50] However, many studies have reported that modification at C-2′, C-7 and/or C-10 of taxanes does indeed modify drug activity.[10,50–56] In this study, the cytotoxicity, evaluated by measurement of the 50% inhibitory concentration (IC_{50}), of unmodified DTX and DTX conjugates was determined in two cancer cell lines (Table 3).

The IC_{50} values for DTX in SKOV3 (1.8 nM) and H460 (1.5 nM) cell lines agreed with previous reports.[36,39] Unfortunately, the cytotoxic effects of **1L-DTX** were much less than those of the parent drug (IC_{50} = 82 or 56 nM; Table 3) and the **2L-** and **3L-DTX** conjugates did not maintain any pharmaceutically relevant cytotoxicity (IC_{50} > 20 μM; Table 3). The superior reactivity of the C-2′ group during acyl-chain conjugation to DTX suggests that the ester group at the C-2′ may be more rapidly hydrolyzed than other conjugation points under biological conditions.[36,52,53,57] Following the 72 h incubation period in RPMI media, a total of 7% ± 2% of the **1L-DTX** was hydrolyzed to produce DTX (1% of **DTX**) and other taxane derivatives. There was no evidence of hydrolysis of the **2L$_{2',7}$-DTX** and **3L-DTX** conjugates.

The proportion of DTX released by hydrolysis of **1L-DTX** within 72 h (1%) is not large enough to completely account for the activity that **1L-DTX** exerted on SKOV3 and H460 cell lines. It remains possible that **1L-DTX** conjugate molecules retain some activity, that other hydrolysis products were also cytotoxic, or that hydrolysis is increased in the presence of the cell lines. Nevertheless, these studies clearly show that the cytotoxicity of **1L-DTX** is significantly impaired in the conjugated form and that this conjugate is slowly hydrolyzed to release the parent drug under biologically relevant conditions.

Similarly, a significant loss in cytotoxicity against the MCF-7 human breast cancer cell line was reported for PTX prodrugs disubstituted at C-2′ and C-7 with acyl chains, of varying lengths (C6:0-C16:0) in comparison to PTX (IC_{50} < 1 nM), due to lack of hydrolysis of the acyl chains.[53] In contrast, mono-substituted bromoacyl-PTX conjugates (IC_{50} values ranged from 3 to 70 nM) were found to retain significantly more of their activity due to ease of hydrolysis of the bromoacyl chains.[53] *In vitro*, PTX prodrugs modified with shorter bromoacyl chains (*i.e.* C6:0-C12:0) were found to be more active than PTX conjugates with longer bromoacyl chains (*i.e.* C14:0–C16:0). In contrast, *in vivo* it was the formulation including 2′-(2-bromo)hexadecanoyl (C16:0, IC_{50} = 70 nM) that was most efficacious, in comparison to liposome formulations incorporating the PTX conjugates with

shorter chain bromoacyl moieties.[53] The authors suggested that the superior efficacy of the formulation incorporating the longer chain bromoacyl PTX conjugate suggests that "slow but sustained delivery" of PTX to tumor cells is advantageous *in vivo*.[53] In light of this information, the **1L-DTX** prodrug in combination with the non-toxic NE formulation, which was shown to circulate for prolonged periods *in vivo* and accumulate preferentially at tumor sites, may be a promising combination.[28,29]

Computational methods

Calculation of hydrophobicity and solubility parameters. QSAR+ and Synthia, Cerius2, Accelrys Inc. (*i.e.* C2_QSAR+ and C2.Synthia)[31] were employed to estimate the octanol to water partition coefficient ($\log P_{o/w}$) and solubility parameters of the compounds, respectively (Table 1). The $\log P_{o/w}$ model employed was established by Ghose and Crippen using the atom-based approach in which each atom is assigned an additive value from a particular class.[32] The C2.Synthia module applies the Fedors approach to calculate the Hildebrand solubility parameters (δ_{HIL}).[33] In a previous study, we examined the accuracy and reliability of various *in silico* methods for use in the selection of a suitable excipient for solubilization of DTX.[9] In this study, the δ_{HIL} values for DTX and a series of excipients were obtained using semi-empirical methods (*i.e.* group contribution method and C2.Synthia module, Cerius^2 software) and molecular dynamics simulation. Overall, the molecular dynamics simulation method produced the most accurate results but required significant time and computational resources. The semi-empirical method, relying on the C2.Synthia module, was found to be fast, reliable and provided a good prediction of the relative degree of solubility of the drug in various structurally similar excipients. For these reasons the C2.Synthia module was employed in the current research to obtain a rapid and straightforward prediction of the δ_{HIL} and log $P_{o/w}$ values.

Theoretically, the smaller the difference between the values for δ_{HIL} of the solute and solvent, the greater the solubility of the solute in the solvent.[33] In this study, the δ_{HIL} values were used to estimate the miscibility of the drugs (*i.e.* DTX conjugates and DTX) and Labrafac™ (*i.e.* tricaprylin and tricaprin) based on the chemical structures of the molecules.[9] The $\log P_{o/w}$ can be employed to predict the relative lipophilicity and retention of the drugs in the inner phase (*i.e.* Labrafac™) of the emulsion formulation.

Experimental

Materials

Anhydrous DTX (99.8%) was obtained from Sai Life Sciences (Hyderabad, India). Lauroyl chloride (98%) and 4-(dimethylamino)pyridine (DMAP) (99%) were purchased from Sigma Aldrich (Oakville, ON, Canada). HPLC-grade solvents were obtained from Caledon (Georgetown, ON, Canada). Labrafac™ (*i.e.* Labrafac™ Lipo WL 1349) and Solutol® (*i.e.* Solutol® HS 15) were provided by Gattefossé Canada, Inc. (Toronto, ON, Canada) and BASF Corporation (Florham Park, NJ), respectively. Gibco® RPMI-1640 medium was acquired from Life Technologies (CA). All materials were used as received.

Synthesis and characterization of DTX conjugates

The conjugation of lauroyl chloride to DTX was monitored by thin layer chromatography (TLC) using chloroform:methanol:hexane (93:3:4, v/v/v) as solvent. The formation of the DTX-conjugates was verified using mass spectrometry (MS) and ^{1}H nuclear magnetic resonance (NMR).

Synthesis. Briefly, DTX (500 mg, 6.19×10^{-4} mol) and DMAP (151.2 mg, 12.38×10^{-4} mol) were dissolved in 15 mL of dichloromethane in a 50 mL round-bottom flask. The reaction mixture was stirred for 10 min under nitrogen atmosphere at 0 °C using an ice bath. Then, lauroyl chloride (147 μL, 6.19×10^{-4} mol) was added dropwise to the mixture followed by stirring for 6 h under nitrogen atmosphere at 0 °C to produce the mono-substituted DTX conjugate, 2′-lauroyl-docetaxel (**1L-DTX**, retention factor (R_f) = 0.20). A second portion of DMAP (151.2 mg, 12.38×10^{-4} mol) and lauroyl chloride (147 μL, 6.19×10^{-4} mol) were added to the reaction mixture and stirred for another 5 h under nitrogen atmosphere at 0 °C. This yielded a mixture of two di-substituted DTX conjugates that were then separated by TLC to obtain the 2′,7-dilauroyl-docetaxel (**2L$_{2',7}$-DTX**, $R_f = 0.70$) and 2′,10-dilauroyl-docetaxel (**2L$_{2',10}$-DTX**, $R_f = 0.60$). Finally, a third portion of DMAP (151.2 mg, 12.38×10^{-4} mol) and lauroyl chloride (147 μL, 6.19×10^{-4} mol) were added to the reaction mixture and stirred for 5 h under nitrogen atmosphere at room temperature to obtain 2′,7,10-trilauroyl-docetaxel (**3L-DTX**, R_f = 0.90).

Purification. The reaction mixture was diluted with diethyl ether, washed with 5% HCl and saline. The solution of DTX conjugate was collected, dried and dissolved in acetonitrile. This solution was then stored at 0 °C overnight followed by filtration to further remove the precipitated impurities. The collected solution was concentrated and applied to a silica gel column with chloroform:methanol:hexane (20 mL of 95:1:4, 20 mL of 94:2:4 and 40 mL of 93:3:4, v/v/v) as mobile phase to obtain the pure DTX conjugates. The yields for the conjugation reactions were greater than 70% in all cases.

Analytical measurements

Nuclear magnetic resonance (NMR) spectroscopy. The ^{1}H NMR spectra were measured with a Mercury 300 spectrometer at 300 MHz in $CDCl_3$. The ^{1}H chemical shifts are reported in Table 2 relative to the internal standard trimethylsilane (^{TM}S) (δ = 0.00 ppm).

Mass spectroscopy. Electrospray Ionization (ESI) was employed on an AB/Sciex QStar mass spectrometer (Applied Biosystems, Foster City, CA) connected to an Agilent 1100 capillary LC system (Agilent Technologies Canada Inc. Mississauga, ON) to determine the chemical composition of the DTX conjugates.

High performance liquid chromatography (HPLC) analysis. The concentration of DTX conjugate and DTX was measured using an HPLC (Agilent series 1200 Liquid Chromatograph, Agilent Technologies Canada Inc. Mississauga, ON) equipped with a Waters UV/VIS detector (Waters Inc., Milford, MA), Agilent sample processor and an Waters XTerra C_{18} reverse-phase column (particle size, 5 μm) of dimensions 4.6 × 250 mm. DTX conjugates and DTX were detected at a wavelength of

227 nm. The flow rate was 1.0 mL/min. The mobile phase used for analysis of DTX (retention time (R_T) = 8 min) was acetonitrile and water (53:47, v/v). Mixtures of 2-propanol, acetonitrile and water (40:45:15, v/v/v) were used to isocratically elute **1L-DTX** (R_T = 5.1 min), **2L$_{2',7}$-DTX** (R_T = 22.4 min) and **2L$_{2',10}$-DTX** (R_T = 20.5 min). The **3L-DTX** was eluted isocratically at 7.0 min and greater than 60 min using 2-propanol:acetonitrile:water with a volume ratio of 74:20:6 and 40:45:15 as mobile phase, respectively.

Dynamic light scattering (DLS). DLS was used to determine the size and distribution of the emulsion at an angle of 90° at room temperature (90Plus Particle Size Analyzer, Brookhaven Instruments Corporation; Holtsville, NY). All samples were measured after 1:400 dilutions using filtered double-distilled water.

Evaluation of relative solubility

The relative solubility of DTX and conjugates (*i.e.* **1L-DTX**, **2L-DTX** and **3L-DTX**) were measured in Labrafac™ at room temperature. Briefly, known amounts of DTX or DTX conjugate were added to Labrafac™ and the mixture was vortexed and stirred at room temperature for 24 h. The samples were then centrifuged in Eppendorf tubes for 1 h at 20000*g* (Eppendorf 5804R, Eppendorf Inc., Hamburg, Germany) to remove undissolved drug. Following centrifugation, the saturated solution (*i.e.* the supernatant) was separated and analyzed by HPLC.[9] The saturation of the solution containing DTX was confirmed by the presence of precipitate on the bottom of the Eppendorf tube. However, precipitate was not observed in the Labrafac™ solutions containing high concentrations of DTX conjugates. The relative solubility of the conjugate in this study, determined by using HPLC, was defined as the concentration of the DTX conjugate in the Labrafac™ unsaturated solution.

Preparation and characterization of the nano-emulsion

Formulations containing low (*i.e.* 0.6% and 1.2% w/w) and high drug concentrations (*i.e.* 5.7% w/w) were prepared and investigated in terms of stability, drug-loading and drug-entrapment efficiency. The compositions of the nano-emulsions (NEs) are provided in Table 4. The NEs were prepared using a slightly modified procedure that was reported in the literature.[34] Briefly, drug (*i.e.* DTX conjugate or DTX) was dissolved and stirred in Labrafac™ at room temperature for 24 h followed by stirring at 60 °C for 10 min. To this solution, Solutol® was added and stirred (630 rpm) for 15 min at 40 °C. The dispersing phase (0.9% w/v NaCl) was then added to this mixture with agitation (840 rpm) and stirred for another 10 min under the same conditions. Finally, the formulation was sonicated for 3 h using a Bransonic 1510 (Bransonic, Danbury, CT). The mean hydrodynamic diameter and size distribution were determined in triplicate by DLS (Table 4). HPLC analysis was used to confirm that the drug and conjugates remained intact following NE preparation. The physical stability of the NE was assessed by size measurements. The NEs were observed under a VWR VistaVision microscope (Mississauga, Ontario, Canada) in order to verify if crystallization of DTX or DTX conjugates had occurred.

Determination of drug loading and entrapment efficiency

The entrapment efficiency (EE) of the NE formulations of DTX or DTX conjugates were measured using both ultracentrifugation and dialysis methods in triplicate.[35]

Ultracentrifugation. Briefly, a 1.0 mL aliquot of an NE sample was placed in the outer chamber of an ultra-filter tube (molecular weight cut-off 10 kDa; Millipore Co., Bedford, USA) and centrifuged at 2500*g* for 1 h at room temperature. The dispersion medium along with the free drug was separated from the NE sample through the ultrafiltration device. The concentration of drug in the dispersion medium (inner chamber) and the supernatant (outer chamber) were measured using HPLC.

Dialysis. The free drug in the dispersion medium was removed using the dialysis method.[35] Briefly, 200 μL of NE sample was added to dialysis tubing (molecular weight cutoff 10 kDa) and suspended in saline (1 L) at room temperature for 40 min. The concentration of drug remaining in the dialysis tubing was measured by HPLC analysis.

Entrapment efficiency was calculated using the following equation:

$$\text{EE}\ (\%) = \frac{\text{Weight of drug in the supernatant or dialysis bag}}{\text{Initial weight of drug loaded}} \times 100 \quad (2)$$

Evaluation of *in vitro* cytotoxicity and hydrolysis

The cytotoxicity of DTX and DTX conjugates were evaluated in triplicate in SKOV-3 human ovarian and H460 human non-small-cell lung cancer cells using RPMI 1640 as cell growth media, as described elsewhere.[36] Briefly, cells were seeded in 96-well plates with a cell density of 5000 cells/well followed by a 24 h incubation period. The cell growth media was then replaced with 150 μL of fresh media containing the appropriate amounts of unmodified DTX, **1L-DTX**, **2L$_{2',7}$-DTX** and **3L-DTX** (n = 3). Following 72 h incubation, the MTT assay was employed to determine the cell viability by measuring optical absorbance at 570 nm using a Spectra Max plus microplate reader (Molecular Devices, Sunnyvale, CA). The cells incubated with drug free media (*i.e.* the control) were considered to be 100% viable.

The hydrolysis of DTX conjugates was studied in RPMI media in triplicate. Briefly, solutions of DTX conjugates (350 μM DTX equivalent) in RPMI were incubated at 37 °C for 72 h. The concentration of DTX, released *via* hydrolysis of the ester bond between the lauroyl moiety and the drug, was measured by HPLC analysis.

Conclusion

This study demonstrates that conjugation of DTX to a moiety that is chemically similar to that of the solubilizing media of the formulation is a promising strategy for enhancing the drug loading and encapsulation efficiency in a NE formulation. However, these studies also highlight the need to consider the impact of chemical modification of a drug on biological activity. Theoretical calculations predicted that the DTX-lauroyl conjugates would have increased solubility in Labrafac™ with the tri-substitute being favored over the di- and mono-substitutes. Indeed,

experimental evaluation revealed that synthesis of the mono-, di- and tri-substituted conjugates resulted in marked increases in the solubility and loading of the drug (in terms of DTX equivalents) in the NE formulation. However, a balance must be achieved between optimizing solubility and maintaining activity. In this regard, the mono-substituted conjugate (**1L-DTX**) is identified as the DTX prodrug with the requisite properties for further consideration.

Acknowledgements

The authors are grateful to the Natural Sciences and Engineering Research Council of Canada (NSERC) for funding this research. JCL acknowledges the Steacie Fellowship from the NSERC and support from the Canada research chair program. L. Huynh thanks Chris Neale for useful discussions regarding the *in vitro* cell culture studies, and Gattefossé Canada Inc. for supplying Labrafac™. Technical assistance from Angel Fu and Laurence Luk is also acknowledged.

References

1 C. A. Lipinski, Drug-like properties and the causes of poor solubility and poor permeability, *J. Pharmacol. Toxicol. Methods*, 2000, **44**, 235–249.
2 L. C. Collins-Gold, R. T. Lyons and L. C. Bartholow, Parenteral emulsions for drug delivery, *Adv. Drug Delivery Rev.*, 1990, **5**, 189–208.
3 P. P. Constantinides, M. V. Chaubal and R. Shorr, Advances in lipid nanodispersions for parenteral drug delivery and targeting, *Adv. Drug Delivery Rev.*, 2008, **60**, 757–767.
4 D. L. Garrec, S. Gori, L. Luo, D. Lessard, D. C. Smith, M.-A. Yessine, M. Ranger and J.-C. Leroux, Poly(N-vinylpyrrolidone)-block-poly(D,L-lactide) as a new polymeric solubilizer for hydrophobic anticancer drugs: *in vitro* and *in vivo* evaluation, *J. Controlled Release*, 2004, **99**, 83–101.
5 T. Negishi, F. Koizumi, H. Uchino, J. Kuroda, T. Kawaguchi, S. Naito and Y. Matsumura, NK105, a paclitaxel-incorporating micellar nanoparticle, is a more potent radiosensitising agent compared to free paclitaxel, *Br. J. Cancer*, 2006, **95**, 601–606.
6 T. Nakanishi, S. Fukushima, K. Okamoto, M. Suzuki, Y. Matsumura, M. Yokoyama, T. Okano, Y. Sakurai and K. Kataoka, Development of the polymer micelle carrier system for doxorubicin, *J. Controlled Release*, 2001, **74**, 295–302.
7 B. B. Lundberg, V. Risovic, M. Ramaswamy and K. M. Wasan, A lipophilic paclitaxel derivative incorporated in a lipid emulsion for parenteral administration, *J. Controlled Release*, 2003, **86**, 93–100.
8 J. Liu, Y. Xiao and C. Allen, Polymer–drug compatibility: A guide to the development of delivery systems for the anticancer agent, ellipticine, *J. Pharm. Sci.*, 2003, **23**, 132–143.
9 L. Huynh, J. Grant, J. C. Leroux, P. Delmas and C. Allen, Predicting the solubility of the anti-cancer agent docetaxel in small molecule excipients using computational methods, *Pharm. Res.*, 2008, **25**, 147–157.
10 M. L. Forrest, J. A. Yãñez, C. M. Remsberg, Y. Ohgami, G. S. Kwon and N. M. Davies, Paclitaxel prodrugs with sustained release and high solubility in poly(ethylene glycol)-b-poly(e-caprolactone) micelle nanocarriers: pharmacokinetic disposition, tolerability, and cytotoxicity, *Pharm. Res.*, 2008, **25**, 194–206.
11 M. O. Bradley, N. L. Webb, F. H. Anthony, P. Devanesan, P. A. Witman, S. Hemamalini, M. C. Chander, S. D. Baker, L. He, S. B. Horwitz and C. S. Swindell, Tumor targeting by covalent conjugation of a natural fatty acid to paclitaxel, *Clin. Cancer Res.*, 2001, **7**, 3229–3238.
12 K. L. Hennenfent and R. Govindan, Novel formulations of taxanes: a review. Old wine in a new bottle?, *Ann. Oncol.*, 2006, **17**, 735–749.
13 J. E. Cortes and R. Pazdur, Docetaxel, *J. Clin. Oncol.*, 1995, **13**, 2643–2655.
14 E. K. Rowinsky and R. C. Donehower, Drug therapy: Paclitaxel (Taxol), *N. Engl. J. Med.*, 1995, **332**, 1004–1014.
15 U.S. National Institutes of Health, http://www.cancer.gov/cancertopics/druginfo/fda-docetaxel, date of access: January 2009.
16 U.S. Food and Drug Administration, http://www.fda.gov/cder/rdmt/internetftap.htm, date of access: January 2009.
17 R. Pazdur, A. P. Kudelka, J. J. Kavanagh, P. R. Cohen and M. N. Raber, The taxoids: paclitaxel (Taxol®) and docetaxel (Taxotere®), *Cancer Treat. Rev.*, 1993, **19**, 351–386.
18 L. B. Michaud, V. Valero and G. Hortobagyi, Risks and benefits of taxanes in breast and ovarian cancer, *Drug Saf.*, 2000, **23**, 401–428.
19 V. Valero, S. F. Jones, D. D. V. Hoff, D. J. Booser, R. G. Mennel, P. M. Ravdin, F. A. Holmes, Z. Rahman, M. W. Schottstaedt, J. K. Erban, L. Esparza-Guerra, R. H. Earhart, G. N. Hortobagyi and H. A. B. 3rd, A phase II study of docetaxel in patients with paclitaxel-resistant metastatic breast cancer, *J. Clin. Oncol.*, 1998, **16**, 3362–3368.
20 J. Crown, M. O'leary and W. S. Ooi, Docetaxel and paclitaxel in the treatment of breast cancer: A review of clinical experience, *The Oncologist*, 2004, **9**(Suppl 2), 24–32.
21 P. G. Rose, J. A. Blessing, H. G. Ball, J. Hoffman, D. Warshal, K. DeGeest and D. H. Moore, A phase II study of docetaxel in paclitaxel-resistant ovarian and peritoneal carcinoma: a Gynecologic Oncology Group study, *Gynecol. Oncol.*, 2003, **88**, 130–135.
22 C. F. Verschraegen, T. Sittisomwong, A. P. Kudelka, E. d. Guedes, M. Steger, T. T. Nelson, M. Vincent, R. Rogers, E. N. Atkinson and J. J. Kavanagh, Docetaxel for patients with paclitaxel-resistant Müllerian carcinoma, *J Clin Oncol.*, 2000, **18**, 2733–2739.
23 L. R. Kelland and G. Abel, Comparative in vitro cytotoxicity of taxol and Taxotere against cisplatin-sensitive and-resistant human ovarian carcinoma cell lines, *Cancer Chemother. Pharmacol.*, 1992, **30**, 444–450.
24 L. Zuylen, J. Verweij and A. Sparreboom, Role of formulation vehicles in taxane pharmacology, *Invest. New Drugs*, 2001, **19**, 125–141.
25 M. Bergh, K. Magnusson, J. L. Nilsson and A. T. Karlberg, Contact allergenic activity of Tween 80 before and after air exposure, *Contact Dermatitis*, 1997, **37**, 9–18.
26 W. B. Shelley, N. Talanin and E. D. Shelley, Polysorbate 80 hypersensitivity, *Lancet*, 1995, **345**, 1312–1313.
27 J. S. Coon, W. Knudson, K. Clodfelter, B. Lu and R. S. Weinstein, Solutol HS 15, nontoxic polyoxyethylene esters of 12-hydroxystearic acid, reverses multidrug resistance, *Cancer Res.*, 1991, **51**, 897–902.
28 J. Rossi, S. Giasson, M. N. Khalid, P. Delmas, C. Allen and J.-C. Leroux, Long-circulating poly(ethylene glycol)-coated emulsions to target solid tumors, *Eur. J. Pharm. Biopharm.*, 2007, **67**, 329–338.
29 M. N. Khalid, P. Simard, D. Hoarau, A. Dragomir and J.-C. Leroux, Long circulating poly(ethylene glycol)-decorated lipid nanocapsules deliver docetaxel to solid tumors, *Pharm. Res.*, 2006, **23**, 752–758.
30 U.S. Food, and Drug Administration, http://www.fda.gov/default.htm, date of access: January 2009.
31 Accelrys Software Inc., Accelrys Software, *Cerius2 Simulation & Prediction, Release 4.6*, Accelrys Software Inc., San Diego, 2001.
32 A. K. Ghose and G. M. Crippen, Atomic physicochemical parameters for three-dimensional structure-directed quantitative structure-activity relationships I. Partition, coefficients as a measure of hydrophobicity, *J. Comput. Chem.*, 1986, **7**, 565–577.
33 R. F. Fedors, A method for estimating both the solubility parameters and molar volumes of liquids, *Polym. Eng. Sci.*, 1974, **14**, 147–154.
34 M. È. Perron, F. Plourde, S. Guérard, L. Huynh, C. Allen and J.-C. Leroux, An investigation on the use of tributyrin nanoemulsions for docetaxel delivery, *J. Drug Del. Sci. Tech.*, 2008, **18**, 189–195.
35 S. R. Dipali, S. B. Kulkarni and G. V. Betageri, Comparative study of separation of non-encapsulated drug from unilamellar liposomes by various methods, *J. Pharm. Pharmacol.*, 1996, **48**, 1112–1115.
36 J. Liu, P. Zahedi, F. Zeng and C. Allen, Nano-sized assemblies of a PEG-docetaxel conjugate as a delivery strategy for docetaxel, *J. Pharm. Sci.*, 2008, **97**, 3274–3290.
37 M. G. Carstens, P. H. J. L. F. d. Jong, C. F. v. Nostrum, J. Kemmink, R. Verrijk, L. G. J. d. Leede, D. J. A. Crommelin and W. E. Hennink, The effect of core composition in biodegradable oligomeric micelles as taxane formulations, *Eur. J. Pharm. Biopharm.*, 2008, **68**, 596–606.
38 T. M. Lima, C. C. Kanunfre, C. Pompéia, R. Verlengia and R. Curi, Ranking the toxicity of fatty acids on Jurkat and Raji cells by flow cytometric analysis, *Toxicol. in Vitro*, 2002, **16**, 741–747.
39 B. T. Hill, R. D. H. Whelan, S. A. Shellard, S. Mcclean and L. K. Hosking, Differential cytotoxic effects of docetaxel in a range of mammalian tumor-cell lines and certain drug-resistant sublines *in-vitro*, *Invest. New Drugs*, 1994, **12**(3), 169–182.

40 M. L. Immordino, P. Brusa, F. Rocco, S. Arpicco, M. Ceruti and L. Cattel, Preparation, characterization, cytotoxicity and pharmacokinetics of liposomes containing lipophilic gemcitabine prodrugs, *J. Controlled Release*, 2004, **100**, 331–336.
41 R. V. Dev, J. M. Babu, K. Vyas, P. S. Ram, P. Ramachandra, N. M. Sekhar, D. N. M. Reddy and N. S. Rao, Isolation and characterization of impurities in docetaxel, *J. Pharm. Biomed. Anal.*, 2006, **40**, 614–622.
42 C. Li, D. F. Yu, R. A. Newman;, F. Cabral, L. C. Stephens, N. Hunter, L. Milas and S. Wallace, Complete regression of well-established tumors using a novel water-soluble poly(L-glutamic acid)-paclitaxel conjugate, *Cancer Res.*, 1998, **58**, 2404–2409.
43 H. Lee, K. Lee and T. G. Park, Hyaluronic acid-paclitaxel conjugate micelles: synthesis, characterization, and antitumor activity, *Bioconjugate Chem.*, 2008, **19**, 1319–1325.
44 H. M. Deutsch, J. A. Glinski, M. Hernandez, R. D. Haugwitz, V. L. Narayanan, M. Suffness and L. H. Zalkow, Synthesis of congeners and prodrugs. 3.[1] Water-soluble prodrugs of taxol with potent antitumor activity, *J. Med. Chem.*, 1989, **32**, 788–792.
45 J. M. G. Cowie, *Polymers: Chemistry and Physics of Modern Materials*, 2nd edn, Nelson Thornes Ltd, Cheltenham, 1991, ch. 8.
46 F. Q. Hu, G. F. Ren, H. Yuan, Y. Z. Du and S. Zeng, Shell cross-linked stearic acid grafted chitosan oligosaccharide self-aggregated micelles for controlled release of paclitaxel, *Colloids Surf., B*, 2006, **50**, 97–103.
47 A. N. Lukyanov and V. P. Torchilin, Micelles from lipid derivatives of water-soluble polymers as delivery systems for poorly soluble drugs, *Adv. Drug Delivery Rev.*, 2004, **56**, 1273–1289.
48 M. Lovreka, B. Zorc, B. Boneschansb and I. Butula, Macromolecular prodrugs. VIII. Synthesis, of polymer–gemfibrozil conjugates, *Int. J. Pharm.*, 2000, **200**, 59–66.
49 Z. Gao, A. N. Lukyanov, A. Singhal and V. P. Torchilin, Diacylpolymer micelles as nanocarriers for poorly soluble anticancer drugs, *Nano Lett.*, 2002, **2**, 979–982.
50 T. Ganesh, Improved biochemical strategies for targeted delivery of taxoids, *Bioorg. Med. Chem.*, 2007, **15**, 3597–3623.
51 J. Parness, D. G. I. Kingston, R. G. Powell, C. Harracksingh and S. B. Horwitz, Structure-activity study of cytotoxicity and microtubule assembly image by taxol and related taxanes, *Biochem. Biophys. Res. Commun.*, 1982, **105**, 1082–1089.
52 E. W. P. Damen, P. H. G. Wiegerinck, L. Braamer, D. Sperling, D. d. Vos and H. W. Scheeren, Paclitaxel esters of malic acid as prodrugs with improved water solubility, *Bioorg. Med. Chem.*, 2000, **8**, 427–432.
53 S. Ali, I. Ahmad, A. Peters, G. Masters, S. Minchey, A. Janoff and E. Mayhew, Hydrolyzable hydrophobic taxanes: synthesis and anti-cancer activities, *Anti-Cancer Drugs*, 2001, **12**, 117–128.
54 T. A. Kirschberg, C. L. VanDeusen, J. B. Rothbard, M. Yang and P. A. Wender, Arginine-based molecular transporters: the synthesis and chemical evaluation of releasable taxol-transporter conjugates, *Org. Lett.*, 2003, **5**, 3459–3462.
55 I. Ojima, S. D. Kuduk, P. Pera, J. M. Veith and R. J. Bernacki, Synthesis and structure-activity relationships of nonaromatic taxoids: effects of alkyl and alkenyl ester groups on cytotoxicity, *J. Med. Chem.*, 1997, **40**, 279–285.
56 W. Mellado, N. F. Magri, D. G. I. Kingston, R. Garcia-Arenas, G. A. Orr and S. B. Horwitz, Preparation and biological activity of taxol acetates, *Biochem. Biophys. Res. Commun.*, 1984, **124**, 329–336.
57 G. Cavallaro, M. Licciardi, P. Caliceti, S. Salmaso and G. Giammona, Synthesis, physico-chemical and biological characterization of a paclitaxel macromolecular prodrug, *Eur. J. Pharm. Biopharm.*, 2004, **58**, 151–159.

